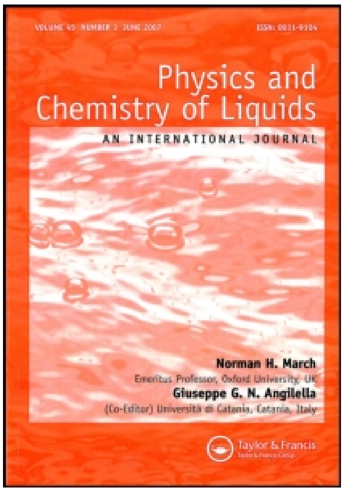

Physics and Chemistry of Liquids
Publication details, including instructions for authors and subscription information:
http://www.informaworld.com/smpp/title~content=t713646857

A Screened Ion—Ion Potential for Liquid Metals Derived from the Green Function Technique

K. Schmidt[a]; W. D. Kraeft[a]; N. H. March[b]
[a] Fachbereich Physik, EMAU Greifswald, Greifswald, Germany [b] Department of Theoretical Chemistry, University of Oxford, Oxford, UK

To cite this Article Schmidt, K. , Kraeft, W. D. and March, N. H.(1991) 'A Screened Ion—Ion Potential for Liquid Metals Derived from the Green Function Technique', Physics and Chemistry of Liquids, 24: 1, 103 — 117
To link to this Article: DOI: 10.1080/00319109108030653
URL: http://dx.doi.org/10.1080/00319109108030653

Phys. Chem. Liq., 1991, Vol. 24, pp. 103–117
Reprints available directly from the publisher
Photocopying permitted by license only

A SCREENED ION–ION POTENTIAL FOR LIQUID METALS DERIVED FROM THE GREEN FUNCTION TECHNIQUE

K. SCHMIDT, W. D. KRAEFT

Fachbereich Physik, EMAU Greifswald, Domstrasse 10a,
Greifswald, D-O-2200, Germany.

and

N. H. MARCH

Department of Theoretical Chemistry, University of Oxford
5 South Parks Road, Oxford, OX1 3UB, UK.

(*Received 6 April 1991*)

Treating a simple liquid metal as a dense two-component plasma consisting of ions and electrons, we derive a rather general screened interionic potential within the framework of the thermodynamic Green function technique. The resulting potential incorporates both ions and electrons into the screening and contains pseudopotential terms of any order. Similar to Hubbard for the electrons, we derive also a static ion local-field correction which accounts for ion–ion correlation effects in the Montroll–Ward approximation. The interionic potential in the case of liquid Cs is strongly modified in comparison with the effective potential derived within second-order pseudopotential theory.

KEY WORDS: Two-component plasma, Green functions, liquid structure

1 INTRODUCTION

One way to obtain a pair potential for liquid metals is to invert measured structure factors as was first done by Johnson and March and Johnson *et al.*[1] In order to derive theoretically an effective ion–ion potential for a liquid metal consisting of ions and nearly free electrons, second-order pseudopotential theory[2] is often used. The result is well known and reads:

$$V_{ii}^{\mathrm{eff}}(r) = \frac{(Ze)^2}{4\pi\varepsilon_0 r} + \int \frac{d\mathbf{q}}{(2\pi)^3} \frac{V_{ei}^2(q)}{V_{ee}(q)} \left[\frac{1}{\varepsilon_{ee}(q,0)} - 1 \right] e^{i\mathbf{q}\cdot\mathbf{r}}, \tag{1}$$

where $V_{ei}(q)$ is a suitable pseudopotential for the electron–ion interaction, $V_{ee}(q)$ describes the pure Coulomb interaction between the electrons and $\varepsilon_{ee}(q, 0)$ is the static dielectric function of the electron sub-system. Nevertheless, the derivation of the potential Eq. (1) "...seems to be rather obscure" according to Abe[3].

Recently, Belyayev, Bobrov and Trigger[4] discussed the quasiparticle spectrum and maxima of dynamic ion structure factors in liquid metals. They considered a liquid metal as a dense two-component plasma and obtained as one result the effective ion–ion potential given above in the framework of the temperature Green functions developed by Abrikosov *et al.*[5].

It has to be mentioned that although the above assumption about the composition of the liquid metal is correct for a simple metal near the melting point, it has been shown experimentally (see e.g. 6 and references quoted therein) that by expanding liquid alkali metals, i.e. by heating the liquids up to the critical point, the systems undergo drastic changes in their electronic properties and a metal–nonmetal transition occurs near the liquid–vapour critical point. This occurrence of the metal–nonmetal transition in expanded liquid alkali metals implies drastic changes in the interatomic forces as the density of the fluid is decreased, especially when the metal–nonmetal transition is approached. Model calculations[7] indicate that these changes are mainly due to atoms or neutral and charged cluster formation, respectively, in the vicinity of the critical point, i.e. drastic changes in the composition of the fluid. In order to construct an effective pair potential for expanded liquid metals, the effects of cluster formation and changes due to the screening of the ion cores should therefore be taken into account.

The aim of this paper is to obtain a general expression for a screened (effective) ion–ion potential for a liquid metal consisting of ions and electrons only (Section 2). One approximation of this expression yields a potential in the form of Eq. (1). Self-consistent to the potential and in the same framework it is possible to derive suitable dielectric functions for the screening such as electron sub-system dielectric functions including the Hubbard[8]—or the Geldart–Vosko local-field correction[9]. In analogy to these electron local-field corrections we construct a simple approximate expression for the ion local-field correction. Section 3 is devoted to some numerical investigations of the screened potentials, derived in Section 2, with respect to different local-field corrections.

2 SCREENED ION–ION POTENTIAL

Regarding a liquid metal as a dense two-component plasma of ions and electrons the thermodynamic Green function technique[10] yields a systematic access to a dynamically screened ion–ion potential. In this framework the derivation of a self-consistent system of equations for the one-particle Green function G, the self energy Σ, the polarization function Π and the screened potential V^s gives the following equation for V^s:

$$V^s_{ab}(12) = V_{ab}(12) + i\hbar \sum_{c,d} \int_0^{-i\hbar\beta} d3\, d4\; V^s_{ac}(13)\,\Pi_{cd}(4343)\,V_{db}(42), \tag{2}$$

where $a \ldots d$ denote the different particle species (ions i, electrons e), 1 stands for the space-time point (r_1, t_1), 2 for (r_2, t_2) and so on, $\beta = 1/K_BT$, and V_{ab} is the corresponding unscreened potential. The sum runs over all species (e, i) and spins (σ_e, σ_i). The polarization function $\cap_{cd}$ has to be determined from the following equation:

$$\cap_{cd}(4343) = -\delta_{cd} G_c(43) G_c(34) - \int_0^{-i\hbar\beta} d1'\, d2'\, G_c(41') \frac{\delta \bar{\Sigma}_c(1'2')}{\delta U_d^{\mathrm{eff}}(33)} G_c(2'4) \tag{3}$$

with

$$U_d^{\mathrm{eff}}(33) = U_d(33) + \Sigma_d^H(33), \tag{4}$$

$$\begin{aligned} \bar{\Sigma}_c(1'2') = \Sigma_c(1'2') - \Sigma_c^H(1'2') &= i\hbar V_{cc}^s(1'2') G_c(1'2') \\ &+ i\hbar \sum_b \int_0^{-i\hbar\beta} d\bar{1}\, d\bar{2}\, V_{cb}^s(1'\bar{2}) G_c(1'\bar{1}) \frac{\delta \bar{\Sigma}_c(\bar{1}2')}{\delta U_b^{\mathrm{eff}}(\bar{2},\bar{2})}, \end{aligned} \tag{5}$$

where Σ_c stands for the full and Σ_c^H for the Hartree self energy, respectively. The effective external field U^{eff} (mean field of interaction) is a sum of the external field U which produces an inhomogeneity in the system and of the Hartree self energy. The one-particle Green function G_c is a solution of the Dyson equation:

$$G_c(11') = G_c^0(11') - \int_0^{-i\hbar\beta} d\bar{1}\, d\bar{2}\, G_c^0(1\bar{1}) \{U_c^{\mathrm{eff}}(\bar{1}, \bar{2}) + \bar{\Sigma}_c(\bar{1}, \bar{2}\} G_c(\bar{2}1'). \tag{6}$$

G_c^0 describes free particles without interaction.

Equation (2) may be expressed by Feynman diagrams.

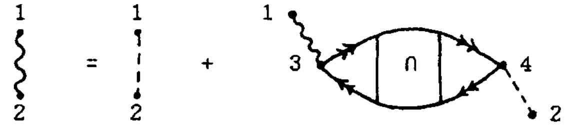

In the thermodynamic equilibrium the quantities V^s, $\cap$ and G are quasiperiodic along the imaginary time axis (Kubo–Martin–Schwinger condition). Therefore, after transition to the momentum Matsubara frequency representation, analytic continuation and considering a potential V_{ab} local in time, i.e. $V_{ab}(12) = V_{ab}(\mathbf{r}_1 - \mathbf{r}_2)\delta(t_1 - t_2)$, we obtain from Eq. (2) with $a = b = i$ (see 10):

$$V_{ii}^s(q, w) = V_{ii}(q) + \hbar \sum_{c,d} V_{ic}^s(q, w) \cap_{cd}(q, w) V_{di}(q). \tag{7}$$

w is a complex frequency which comes from the analytic continuation of the functions V^s and $\cap$ into the complex frequency-plane (Bose-like Matsubara frequencies $\Omega_v = i\pi v/\hbar\beta$; $v = 0, \pm 2, \pm 4, \ldots$; $\Omega_v \to w$). $\hbar q$ denotes the particle momentum.

It is obvious that an additional equation for the screened ion–electron potential

V^s_{ie} is needed to determine V^s_{ii} in Eq. (7). In analogy to (7) one obtains from (2) for V^s_{ie}:

$$V^s_{ie}(q, w) = V_{ie}(q) + \hbar \sum_{c,d} V^s_{ic}(q, w) \bigcap\nolimits_{cd}(q, w) V_{de}(q). \tag{8}$$

Inserting (8) into (7) and rearranging the resulting equation with respect to $V^s_{ii}(q, w)$, yield a general expression for the dynamically screened ion–ion potential for liquid metals which is modified on account of many-particle effects and which contains V_{ie}-powers of any order because of the nonvanishing polarization functions. This can easily be seen from the equation obtained (here without spin summation)

$$V^s_{ii}(q, w) = \{V_{ii}(q)*[1 - \hbar V_{ee}(q)\bigcap\nolimits_{ee}(q, w)] + \hbar V_{ie}(q)V_{ei}(q)\bigcap\nolimits_{ee}(q, w)\}/F(q, w) \tag{9}$$

$$\begin{aligned} F(q, w) = 1 &- \hbar V_{ii}(q)\bigcap\nolimits_{ii}(q, w) - \hbar V_{ee}(q)\bigcap\nolimits_{ee}(q, w) - \hbar v_{ei}(q)\bigcap\nolimits_{ie}(q, w) - \hbar V_{ie}(q)\bigcap\nolimits_{ei}(q, w) \\ &+ \hbar^2 V_{ii}(q)V_{ee}(q)*[\bigcap\nolimits_{ii}(q, w)\bigcap\nolimits_{ee}(q, w) - \bigcap\nolimits_{ei}(q, w)\bigcap\nolimits_{ie}(q, w)] \\ &+ \hbar^2 V_{ei}(q)V_{ie}(q)*[\bigcap\nolimits_{ei}(q, w)\bigcap\nolimits_{ie}(q, w) - \bigcap\nolimits_{ii}(q, w)\bigcap\nolimits_{ee}(q, w)] \end{aligned}$$

and after expanding the denominator $F(q, w)$ in powers of $V_{ei}(q)$ or $V_{ie}(q)$, respectively. Note that for a system in which the ions and electrons interact via pure Coulomb potentials, i.e.

$$V_{ii}(q) = -ZV_{ei}(q) = -ZV_{ie}(q) = Z^2 V_{ee}(q) = \frac{(Ze)^2}{\varepsilon_0 q^2} \tag{10}$$

(Z—charge number), (9) reads as follows:

$$V^s_{ii}(q, w) = \frac{V_{ii}(q)}{\varepsilon(q, w)} \tag{11}$$

with the liquid metal dielectric function

$$\varepsilon(q, w) = 1 - \hbar \sum_{a,b} V_{ab}(q)\bigcap\nolimits_{ab}(q, w), \; (a, b = e, i). \tag{12}$$

In order to solve (9) including spin summation one has to solve the whole self-consistent system of the Eqs. (2), (3), (5) and (6) approximately to obtain a screened (effective) potential that contains the main effects in simple liquid metals such as strong electron correlations, degeneracy and ion-core effects.

The first approximation that can be chosen was given by Belyayev *et al.*[4]. According to the pseudopotential theory[2] (weak ion–electron interaction, nearly free electron model), the contribution of the polarization functions $\bigcap_{ei}(q, w)$ and $\bigcap_{ie}(q, w)$ can be neglected. In this way an expression for $V^s_{ii}(q, w)$ from (9) with $V_{ie}(q) = V_{ei}(q)$ and including spin summation is obtained which is still more general than (1).

$$V_{ii}^{s}(q, w) = \frac{V_{ii}(q)\varepsilon_{ee}(q, w) + \dfrac{V_{ei}^{2}(q)}{V_{ee}(q)}[1 - \varepsilon_{ee}(q, w)]}{\varepsilon_{ii}(q, w)\varepsilon_{ee}(q, w) - \dfrac{V_{ei}^{2}(q)}{V_{ii}(q)V_{ee}(q)}[1 - \varepsilon_{ii}(q, w)][1 - \varepsilon_{ee}(q, w)]}. \tag{13}$$

Here we have used the following abbreviation for the ion and electron polarizabilities which corresponds to the usual dielectric function for sub-systems of electrons or ions, respectively ($a = e, i$):

$$\varepsilon_{aa}(q, w) - 1 \equiv -\hbar(2\sigma_a + 1)V_{aa}(q)\Pi_{aa}(q, w). \tag{14}$$

Introducing the approximation $\Pi_{ii}(q, w) = 0$ into (13), a screened potential in Fourier space in the form of (1) is derived immediately:

$$V_{ii}^{s}(q, w) = V_{ii}(q) + \frac{V_{ei}^{2}(q)}{V_{ee}(q)}\left[\frac{1}{\varepsilon_{ee}(q, w)} - 1\right], \tag{15}$$

where dynamic effects are still taken into account because of the w-dependence of the dielectric function.

In the Appendix, we show how electron–elelectron and ion–ion polarizabilities can be derived consistently within the framework adopted above. Below, we shall present some results for interionic potentials for different thermodynamic states.

3 STATIC DIELECTRIC FUNCTIONS AND EFFECTIVE INTERIONIC PAIR POTENTIALS FOR LIQUID Cs

First we note that the static RPA polarization function for noninteracting particles is given by[12]:

$$\Pi_{aa}^{\mathrm{RPA}}(q, 0) = \frac{1}{\hbar}\int \frac{dk}{(2\pi)^3}\,\frac{f_a(k) - f_a(k + q)}{E_a(k) - E_a(k + q) + i\hbar\mu},\ \mu \to 0 \tag{16}$$

($a = e, i$), with $f_a(k)$ and $E_a(k)$ representing the Fermi function and the kinetic energy, respectively. Under completely degenerate conditions ($T = 0$ K), as is approximately the case for metal electrons in the vicinity of the melting point, Π_{ee}^{RPA} reduces to:

$$\Pi_{ee}^{\mathrm{RPA}}(q, 0) = -\frac{m_e}{2\pi^2\hbar^3}\,q_F\left[\frac{1}{2} + \frac{4q_{F^2} - q^2}{8qq_F}\ln\left(\frac{2q_F + q}{2q_F - q}\right)\right] \tag{17}$$

(q_F—Fermi wave number; m_e—electron mass). Because of their higher mass compared with electrons, the metal ions represent, in the density-temperature region from the melting up to the liquid–vapour critical point, classical nondegenerate particles. Thus, Eq. (16) yields for the ion–ion polarization function[13]:

$$\Pi_{ii}^{\mathrm{RPA}}(q, 0) = -\frac{1}{(2\sigma_i + 1)} \frac{\beta n_i}{\hbar} \, {}_1F_1\left[1, \frac{3}{2}; -\frac{\beta \hbar^2 q^2}{8 m_i}\right] \tag{18}$$

(${}_1F_1$—confluent hypergeometric function; m_i—ion mass; n_i—ion number density). For simplicity, $\sigma_i = 0$ was taken in all calculations.

Using the relations (16)–(18) we have investigated the different polarizabilities and screened ion–ion potentials for liquid Cs at its melting point ($T_m = 301.55$ K, $\rho_m = 1.8355$ g/cm^3, $r_s = 5.786$; $r_s = d/a_0$, $d = (3/4\,\pi n_i)^{1/3}$, $a_0 = \hbar^2\, 4\pi\varepsilon_0/m_e e^2$). Here the assumption of Cs$^+$ ions ($Z = 1$) and electrons is entirely realistic. Although this assumption, as discussed above, is by no means as well established at lower densities, it has proved useful, for comparison purposes, to carry out calculations on the basis of it also near the critical point[8] ($T = 1923$ K, $\rho = 0.59$ g/cm^3, $r_s = 8.446$).

Based on the Appendix, we have first calculated, for better comparison with the results of other authors, the inverse static dielectric functions $1/\varepsilon_{ee}(q, 0)$ (curves 1–4 of Figures 1 and 2) and $1/\varepsilon_{ii}(q, 0)$ (curves 5–6) for the two thermodynamic states discussed immediately above.

The different curve numbers denote different local-field corrections (1—Hubbard[8], Eq. (A9); 2—Geldart and Vosko[9], Eq. (A10); 3—RPA ($g_e(q) = 0$); 4—fitting formula

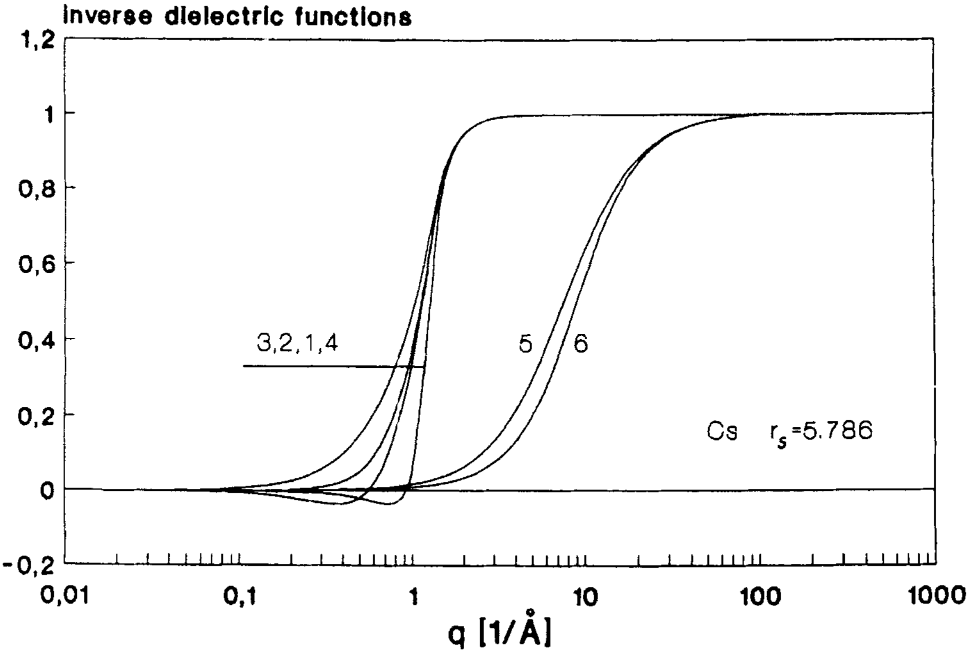

Figure 1 Inverse static electronic and ionic dielectric functions $1/\varepsilon_{ee}(q, 0)$ (curves 1–4) and $1/\varepsilon_{ii}(q, 0)$ (curves 5–6) for $r_s = 5.786$ with respect to different local-field corrections: 1—Hubbard[8]; 2—Geldart and Vosko[9]; 3—RPA ($g_e(q) = 0$); 4—fitting formula by Ichimaru and Utsumi[11]; 5—RPA ($g_i(q) = 0$); 6—formula (A21) of the present paper with $\sigma_i = 0$.

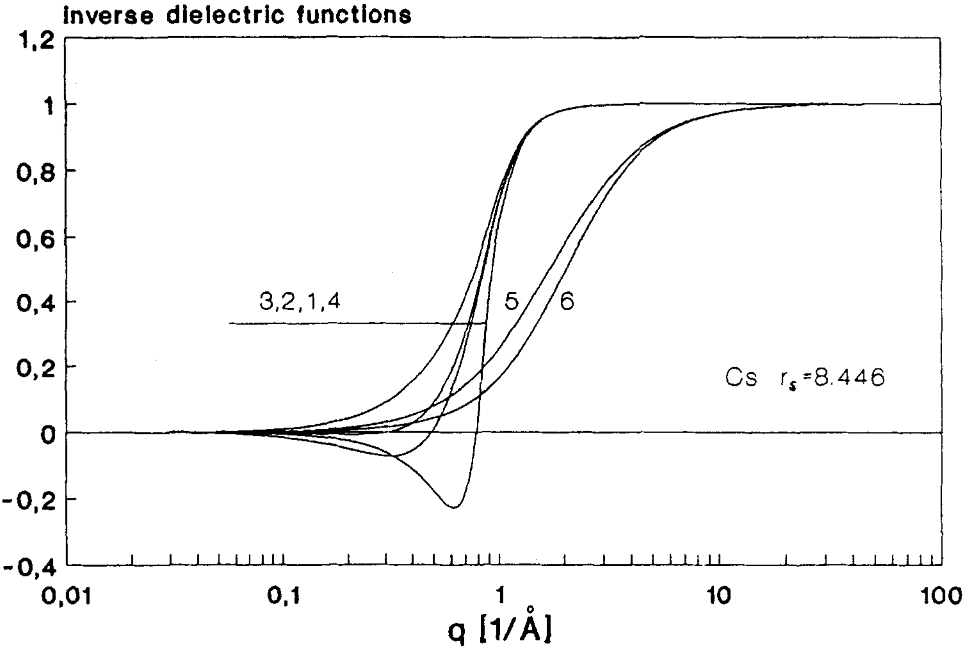

Figure 2 Inverse static electronic and ionic dielectric functions $1/\varepsilon_{ee}(q, 0)$ (curves 1–4) and $1/\varepsilon_{ii}(q, 0)$ (curves 5–6) for $r_s = 8.446$ with respect to different local-field corrections (notation as in Figure 1).

of Ichimaru and Utsumi[11]; 5—RPA ($g_i(q) = 0$); 6—formula (A21) of the present paper). The differences between the electron and ion sub-system dielectric functions come from the different masses as well as from the different local-field corrections just cited.

Turning to the effective ion–ion potentials, calculations have been made using the Ashcroft empty core potential[14] in all cases. At the melting point R_c was taken as 1.435 Å while near the critical point R_c was chosen to be 2.166 Å.

At the melting point, the main conclusion, based on the Fourier transform of Eq. (15), is that the statically screened interionic potential for Cs is very sensitive to the changes in the electronic screening functions (see e.g. 15 in the case of all alkali metals). Thus, RPA gives practically no binding in the effective ion–ion potential $V^s_{ii}(r)$, Geldart and Vosko[9] a minimum at 5.7 Å with a depth of −0.04 eV, the Ichimaru and Utsumi[11] prescription moves the minimum inwards to 5.3 Å and deepens the potential just slightly. The deepest potential $V^s_{ii}(r)$ we calculated at the melting point comes from Hubbard[8] screening (depth −0.1 eV, minimum at 5.3 Å).

The features near the liquid–vapour critical point are similar to those at the melting point. RPA gives practically no binding, Geldart and Vosko[9] yields a minimum of −0.04 eV at 8.0 Å, Ichimaru and Utsumi[11] a minimum at 7.6 Å with a depth of −0.05 eV and Hubbard[8] deepens the potential to −0.08 eV at the same position (7.6 Å).

Note that the ion–ion potential $V^s_{ii}(r)$, based on the Fourier transform of Eq. (13)

including the ion local-field correction (A21) and the Ichimaru and Utsumi electron screening[11], produces a minimum of -0.02 eV at 2.4 Å near the critical point whereas it gives a potential depth of -0.09 eV at 0.5 Å at the melting point.

While, unfortunately, the available approximate structural theories are not sufficiently accurate (though for refinement see below) for quantitative answers[18], nevertheless at $T = 1923$ K they give minima near 5.5 Å and depths of -0.05 to -0.06 eV (see 16). In the discussion in Section 4 below, we shall comment on the relation to the 'diffraction' potential $\Phi(r)$ obtained by inverting the structure factor $S(q)$ as measured by Hensel *et al.*[6].

4 DISCUSSION AND SUMMARY

In order to investigate separately the contributions of the ions and electrons to the screening of the effective ion–ion potential (13), we have additionally evaluated the potential

$$V_{ii}^{s}(q, 0) = \frac{V_{ii}(q)}{\varepsilon_{ii}(q, 0)}, \tag{19}$$

where the electronic screening is neglected and $\varepsilon_{ii}(q, 0)$ is given by Eq. (A20). It is then found that the electrons determine mainly the long-range part of the ion–ion interaction (Friedel oscillations) whereas the effective collision diameter remains relatively unchanged, i.e. the short-range part of the ion–ion interaction is determined by the ions themselves.

At the melting point, the ion cores and potential wells, calculated with Eqs (13) and (19), are nearly the same. The differences between these two potentials increase gradually with increasing temperature and decreasing density. It is therefore very likely that, by using (13), the ions are overestimated in the screening mechanism. We believe that their contribution could be compensated to a certain extent by the neglected terms $\bigcap_{ei}$ and $\bigcap_{ie}$. The latter should be investigated in detail.

A comparison of Figures 1 and 2 (see Figure 3) indicates that the inverse ion and electron sub-system dielectric functions approach each other and move to smaller wave numbers q with increasing temperature and decreasing density. Thus, in a high temperature–high density plasma region of several thousand Kelvin and densities about 10^{16}–10^{18} per cm^3 the differences between the potentials (13) and (15) vanish gradually.

It is also relevant to note here that the consideration of the ion spin σ_i leads only to a prefactor in the ion local-field correction which causes a shifting of the function $1/\varepsilon_{ii}(q, 0)$ to the corresponding RPA expression (curve 5 in Figures 1 and 2) and therefore to a shifting of the screened interionic potential (13) such that the effective collision diameter becomes larger and the potential depth smaller.

In conclusion, let us return to the relation between electron theory and diffraction $\Phi(r)$'s. For one case, liquid metal sodium just above its freezing point, Perrot and March[18] have brought electron theory into direct contact with the diffraction

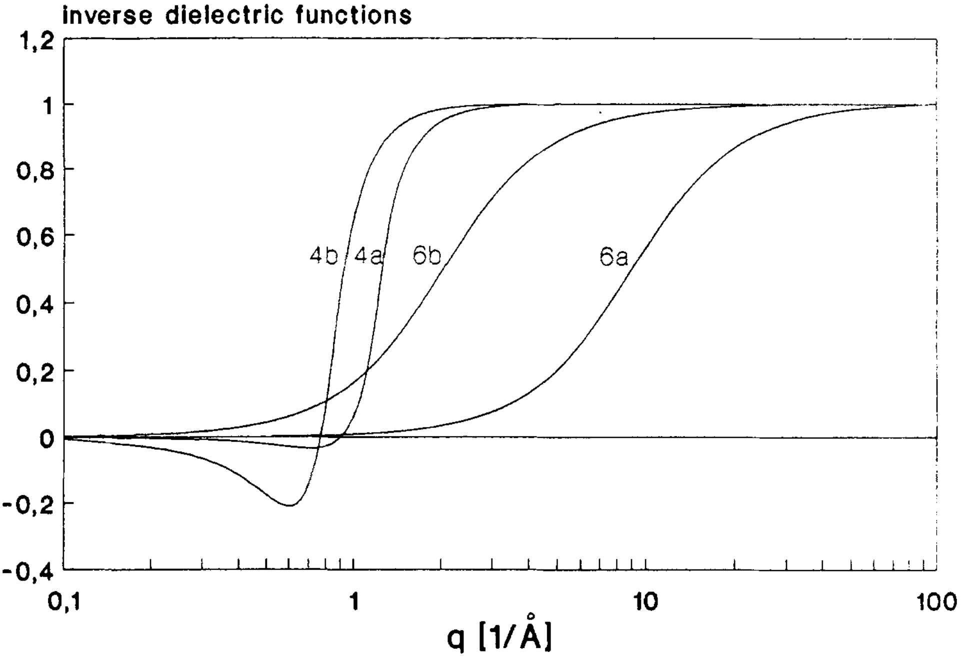

Figure 3 Inverse static dielectric functions $1/\varepsilon_{ee}(q, 0)$ with the electron local-field correction according to Ichimaru and Utsumi[11] (curves 4a and 4b) and $1/\varepsilon_{ii}(q, 0)$ with the ion local-field correction according to formula (A21) ($\sigma_i = 0$) of the present paper (curves 6a and 6b) at $r_s = 5.786$ (a) and $r_s = 8.446$ (b).

potential obtained by Reatto *et al.*[19]. In the work of Reatto *et al.*, the important new step was to transcend approximate liquid structural theories by employing computer simulation to iterate to the 'final diffraction potential'. It is worth noting also, in connection now with electron theory, that for liquid Na, and also in unpublished work[20] on K near freezing, that the method of Perrot and March has avoided uncertainties in the choice of a pseudopotential by solving for the displaced valence electron screening charge around a Na^+ or K^+ ion embedded in an originally uniform bath of electrons of densities appropriate to these two liquid metals at freezing. The input information here, in addition to these densities from experiment, was the atomic number (e.g. 11 for Na) and a prescription in a local density approximation for the exchange and correlation potential $V_{xc}(r)$. All the main features of the diffraction potential of Reatto *et al.* for liquid Na at freezing were reproduced by the electron theory $\Phi(r)$ of Perrot and March.

However, we are still some way from making such comparisons for the heavy liquid alkali metal Cs considered here. It therefore remains of considerable interest to attempt to 'tighten up' considerations on (a) the choice of pseudopotential, (b) the choice of electronic screening functions within the framework proposed here based on Eq. (15) and (c) the 'fine tuning' of $\Phi(r)$ which might possibly arise from contributions from ion screening. In connection with (c), we believe that with the approximations we have developed to date, ion screening is overemphasized. Therefore, it seems clear that the main difficulties in applying the present theory to liquid metal Cs and its effective ion–ion potential still rest on the uncertainties (a) and (b) noted immediately above.

Acknowledgements

One of the authors (K. S.) would like to thank Prof. F. Hensel and Dr. R. Winter (Marburg) for hospitality at the Institut for Physical Chemistry and for many useful discussions. Another of us (N. H. M.) is grateful to Mr. J. A. Ascough for numerus valuable discussions on the usefulness of 'diffraction' potentials for Cs along the liquid–vapour coexistence curve, obtained by inversion of the measured $S(q)$'s using approximate liquid structural theories.

APPENDIX: ELECTRON–ELECTRON AND ION–ION POLARIZATION FUNCTION

In the Appendix we want to give a derivation of the electron polarizability $\varepsilon_{ee}(q, w) - 1$ for strongly correlated and highly degenerate electron liquids at metallic densities, where $r_s \geq 1$, including the Hubbard[8] and the Geldart–Vosko local-field correction[9] in the framework of the thermodynamic Green function technique[10]. This study yields an insight into the procedure of the derivation of local-field corrections which is useful for the construction of an ion polarizability.

Since the Fermi energy of the electrons is much greater than the thermal energy of the ions in many of the practical cases, we may invoke the adiabatic approximation for the motion of the electrons, so that only the static part $\varepsilon_{ee}(q, 0)$ enters the screening of the interionic potential (see 11).

The starting point of our considerations is Eq. (3) for the polarization function $\Pi_{ee}(4343)$ of the electron sub-system. At metallic densities one attempts to go beyond the RPA, which is given by the first term on the right-hand side of (3), by taking account of exchange and Coulomb correlation effects via the electron self energy $\Sigma_e(1'2')$. The schemes proposed by Hubbard[8] and Geldart and Vosko[9] consider exchange effects only. This corresponds to the Hartree–Fock approximation $\Sigma_e^{\mathrm{HF}}(1'2')$ of the self energy in (5), where the integral term is therefore neglected and the screened electron–electron potential is replaced by an unscreened one.

$$\Sigma_e(1'2') \approx \Sigma_e^{\mathrm{HF}}(1'2') = i\hbar V_{ee}(1'2')G_e(1'2') =$$

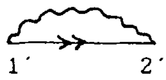

. (A1)

The functional derivative of the Hartree–Fock self energy (A1) with respect to the effective external field $U_e^{\mathrm{eff}}(33)$ (vertex function) yields from (3), together with the definition of the electron–electron polarization function[10]

$$\Pi_{ee}(1'32'3) \equiv -\frac{\delta G_e(1'2')}{\delta U_e^{\mathrm{eff}}(33)}, \tag{A2}$$

an integral equation for the latter:

$$\Pi_{ee}(4343) = -G_e(43)G_e(34) + i\hbar \int_0^{-i\hbar\beta} d1'\, d2'\, G_e(41')V_{ee}(1'2')\Pi_{ee}(1'3\ 2'3)G_e(2'4). \tag{A3}$$

The iterative solution of this integral equation can be expressed by Feynman diagrams and reads:

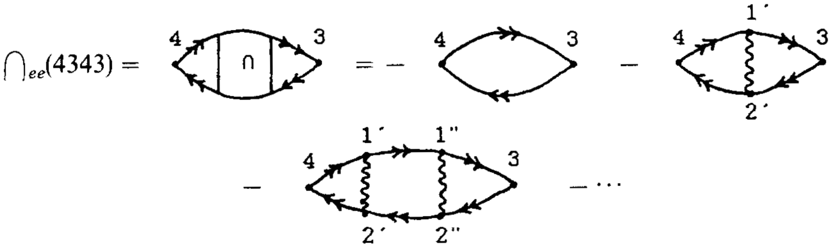

(A4)

After transition to the momentum Matsubara frequency representation and identifying the potentials in (A4) to be Coulombic, each potential line corresponds to:

$$V_{ee}(|\mathbf{q}+\mathbf{k}_1 - \mathbf{k}_2|) = \frac{e^2}{\varepsilon_0 |\mathbf{q} + \mathbf{k}_1 - \mathbf{k}_2|^2}, \tag{A5}$$

where $\mathbf{k}_1$ and $\mathbf{k}_2$ designate the wave vectors of the two incoming electrons, characterized by Green function lines, into each vertex. The estimate of the potential $V_{ee}(|\mathbf{q} + \mathbf{k}_1 - \mathbf{k}_2|)$ by approximate potentials $V_{ee}^{\mathrm{Hu}}(q)$ or $V_{ee}^{\mathrm{GV}}(q)$, given by

$$V_{ee}^{\mathrm{Hu}}(q) = \frac{e^2}{\varepsilon_0(q^2 + q_F^2)} \quad \text{and} \quad V_{ee}^{\mathrm{GV}}(q) = \frac{e^2}{\varepsilon_0(q^2 + 2q_F^2)}, \tag{A6}$$

finally leads to the Hubbard[8] or Geldart–Vosko local-field corrections[9], respectively. By the use of the k_1 and k_2-independent potentials (A6) instead of (A5), each "bubble" in (A4) of the order n splits simply into two contributions in Fourier space:

$$[-\hbar V'_{ee}(q)]^n * [\Pi_{ee}^{\mathrm{RPA}}(q, \Omega_v)]^{n+1}$$

with $V'_{ee}(q) = V_{ee}^{\mathrm{Hu}}(q)$ or $V_{ee}^{\mathrm{GV}}(q)$, respectively. Here, n denotes the potential line number ($n = 0 \ldots \infty$). Thus, one obtains for the electron–electron polarization function after analytic continuation $(\Omega_v \rightarrow w)$[8]:

$$\Pi_{ee}(q, w) = \frac{\Pi_{ee}^{\mathrm{RPA}}(q, w)}{1 + \hbar V'_{ee}(q)\Pi_{ee}^{\mathrm{RPA}}(q, w)}. \tag{A7}$$

Inserting (A7) into the definition (14) and treat the static case ($w = 0$) as mentioned above, the electron polarizability according to Hubbard[8] or Geldart and Vosko[9] is readily obtained, which accounts for electron exchange effects via the corresponding local-field corrections $g_e(q) = g_e^{\mathrm{Hu}}(q)$ or $g_e^{\mathrm{GV}}(q)$, respectively:

$$\varepsilon_{ee}(q, 0) - 1 = -\frac{\hbar(2\sigma_e + 1)V_{ee}(q)\Pi_{ee}^{\mathrm{RPA}}(q, 0)}{1 + \hbar(2\sigma_e + 1)V_{ee}(q)\Pi_{ee}^{\mathrm{RPA}}(q, 0)g_e(q)} \tag{A8}$$

with

$$g_e^{\mathrm{Hu}}(q) = \frac{1}{(2\sigma_e + 1)}\frac{V_{ee}^{\mathrm{Hu}}(q)}{V_{ee}(q)} = \frac{q^2}{2(q^2 + q_F^2)} \tag{A9}$$

and

$$g_e^{\mathrm{GV}}(q) = \frac{1}{(2\sigma_e + 1)}\frac{V_{ee}^{\mathrm{GV}}(q)}{V_{ee}(q)} = \frac{q^2}{2(q^2 + 2q_F^2)}. \tag{A10}$$

Note, that in RPA $g_e(q) = 0$, and with T = 0K the polarizability (A8) is reduced to the Lindhard[12] one.

In principle, local-field corrections that include also electron correlation effects can be derived in the same manner as was demonstrated for the Hubbard[8] or Geldart and Vosko[9] one. This implies, however, to choose at least the V^s-approximation[10] for the electron self energy

$$\bar{\Sigma}_e(1'2') \approx i\hbar V_{ee}^s(1'2')G_e(1'2') =$$

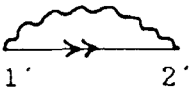

instead of the Hartree–Fock approximation (A1).

In contrast to the electrons, the liquid metal ions behave as classical particles. Therefore, one has to choose approximations for the ion self energy (5) which go beyond the Hartree–Fock approximation. For this purpose we start with the V^s-approximation[10] just cited

$$\bar{\Sigma}_i(1'2') \approx \bar{\Sigma}_i^{\mathrm{HF}}(1'2') + \bar{\Sigma}_i^{\mathrm{MW}}(1'2') = i\hbar V_{ii}^s(1'2')G_i(1'2'), \tag{A11}$$

the vertex function of which is given by

$$\frac{\delta\bar{\Sigma}_i(1'2')}{\delta U_i^{\mathrm{eff}}(33)} = i\hbar\left[G_i(1'2')\frac{\delta V_{ii}^s(1'2')}{\delta U_i^{\mathrm{eff}}(33)} - V_{ii}^s(1'2')\Pi_{ii}(1'3\;2'3)\right]. \tag{A12}$$

$\bar{\Sigma}_i^{\mathrm{MW}}$ denotes the ionic Montroll–Ward contribution. Neglecting the first term of the right-hand side of (A12), i.e. dropping contributions to the vertex function of higher order than linear in V_{ii}^s, yields the following equation for the ion–ion polarization function Π_{ii}:

$$\Pi_{ii}(4343) = -G_i(43)G_i(34) + i\hbar\int_0^{-i\hbar\beta} d1'\,d2'\;G_i(41')V_{ii}^s(1'2')\Pi_{ii}(1'3\;2'3)G_i(2'4). \tag{A13}$$

Namely, taking the simplest approximation for $\bigcap_{ii}$ in (3), i.e. RPA for ideal noninteracting particles

$$\bigcap_{ii}(4343) = -G_i^0(43)G_i^0(34), \tag{A14}$$

from Eq. (2) it follows (see 17) that

$$\frac{\delta V_{ii}^s(1'2')}{\delta U_{\mathrm{i}}^{\mathrm{eff}}(33)} = -i\hbar(2\sigma_i + 1)\int_0^{-i\hbar\beta} d4\ d5\ V_{ii}^s(1'4)V_{ii}^s(52')$$
$$* \left[G_i^o(53)G_i^0(34)G_i^0(45) + G_i^0(54)G_i^0(43)G_i^0(35)\right] \tag{A15}$$

which is already a quadratic function in V_{ii}^s. Inserting (A15) into (A12) yields therefore a contribution to the vertex function quadratic in V_{ii}^s.

The iterative solution of the integral Eq. (A13) is similar to (A4):

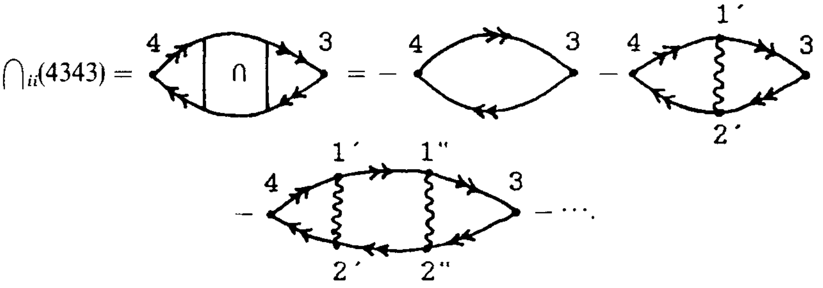

(A16)

Now, one should insert (A16) into the equation for the screened ion–ion potential (2) and solve the resulting equation. However, in order to obtain a compact expression for $\bigcap_{ii}$ from (A16) in the form of (A7), one has to estimate the screened potentials V_{ii}^s in (A16) by a suitable potential as was done for the unscreened electron–electron potentials (A5). Therefore, we propose to replace the screened ion–ion potentials in (A16) after transition to the momentum Matsubara frequency representation by static Debye potentials:

$$V_{ii}^s(\mathbf{q} + \mathbf{k}_1 - \mathbf{k}_2) = \frac{(Ze)^2}{\varepsilon_0(|\mathbf{q} + \mathbf{k}_1 - \mathbf{k}_2|^2 + \kappa_D^2)}, \quad \kappa_D^2 = \frac{(Ze)^2 n_i}{\varepsilon_0 K_B T}. \tag{A17}$$

Now, $\mathbf{k}_1$ and $\mathbf{k}_2$ denote the wave vectors of the two incoming ion Green function lines into each vertex of (A16). In analogy to the Hubbard local-field correction[8] for the electrons, we approximate the potential (A17), in the next step, by the following $\mathbf{k}_1$ and $\mathbf{k}_2$-independent potential:

$$V_{ii}^{s'}(q) = \frac{(Ze)^2}{\varepsilon_0((q^2 + \kappa_D^2) + \kappa_D^2)} = \frac{(Ze)^2}{\varepsilon_0(q^2 + 2\kappa_D^2)}, \tag{A18}$$

which has a formal similarity to the corresponding Geldart–Vosko expression (A6). Using the modified screened potential (A18) in (A16), each 'bubble' of the order n

splits into two contributions in Fourier space:

$$[-\hbar V^{s'}_{ii}(q)]^{n} * [\Pi^{\mathrm{RPA}}_{ii}(q, \Omega_{\nu})]^{n+1}$$

where n denotes again the potential line number ($n = 0 \ldots \infty$). In this way, we obtain the desired compact equation for the ion–ion polarization function from (A16) after analytic continuation ($\Omega_{\nu} \to w$) and in the static case ($w = 0$):

$$\Pi_{ii}(q, 0) = \frac{\Pi^{\mathrm{RPA}}_{ii}(q, 0)}{1 + \hbar V^{s'}_{ii}(q)\Pi^{\mathrm{RPA}}_{ii}(q, 0)}. \tag{A19}$$

Inserting (A19) into (14) yields finally an ion polarizability which takes care of correlation effects between ions in the Montroll–Ward approximation:

$$\varepsilon_{ii}(q, 0) - 1 = -\frac{\hbar(2\sigma_i + 1)V_{ii}(q)\Pi^{\mathrm{RPA}}_{ii}(q, 0)}{1 + \hbar(2\sigma_i + 1)V_{ii}(q)\Pi^{\mathrm{RPA}}_{ii}(q, 0)g_i(q)}. \tag{A20}$$

Here, we have introduced the following definition for the ion local-field correction $g_i(q)$ in analogy to (A9) or (A10):

$$g_i(q) \equiv \frac{1}{(2\sigma_i + 1)} \frac{V^{s'}_{ii}(q)}{V_{ii}(q)} = \frac{1}{(2\sigma_i + 1)} \frac{q^2}{(q^2 + 2\kappa_D^2)}. \tag{A21}$$

References

1. M. D. Johnson and N. H. March, *Phys. Lett.*, **3**, 313 (1963); M. D. Johnson, P. Hutchinson and N. H. March, *Proc. Roy. Soc. London*, **A282**, 283 (1964).
2. W. A. Harrison, *Pseudopotentials in the Theory of Metals*, Benjamin, New York (1966).
3. R. Abe, *J. Phys. Soc. Jpn.*, **58**, 918 (1989).
4. A. M. Belyayev, V. B. Bobrov and S. A. Trigger, *J. Phys.: Condens. Matter*, **1**, 9665 (1989).
5. A. A. Abrikosov, L. P. Gorkov and I. E. Dzialoszynski, *Methods of Quantum Field Theory in Statistical Physics*, Moscow: GIFML (in Russian) (1962).
6. R. Winter and F. Hensel, *Phys. Chem. Liq.*, **20**, 1 (1989); F. Hensel and H. Uchtmann, *Annu. Rev. Phys. Chem.*, **40**, 61 (1989).
7. R. Redmer and G. Röpke, *Contrib. Plasma Phys.*, **29**, 343 (1989); V. V. Gogoleva, V. Yu. Zitserman, A. Ya. Polishuk and I. T. Iakubov, *Teplofiz. Vys. Temp.*, **22**, 208 (1984); J. P. Hernandez, *Phys. Rev. Lett.*, **53**, 2320 (1984); **57**, 3183 (1986); *Phys. Rev.*, **A31**, 932 (1985); **A34**, 1316 (1986).
8. J. Hubbard, *Proc. Roy. Soc. London*, **A243**, 336 (1958).
9. D. J. W. Geldart and S. H. Vosko, *Can. J. Phys.*, **44**, 2137 (1966).
10. P. C. Martin and J. Schwinger, *Phys. Rev.*, **115**, 1342 (1959); L. Kadanoff and G. Baym, *Quantum Statistical Mechanics*, Benjamin, New York (1962); W. D. Kraeft, D. Kremp, W. Ebeling and G. Röpke, *Quantum Statistics of Charged Particle Systems*, Akademie-Verlag, Berlin (1986); Plenum, London/New York (1986).
11. S. Ichimaru and K. Utsumi, *Phys. Rev.*, **B24**, 7385 (1981); K. Utsumi and S. Ichimaru, *Phys. Rev.*, **A26**, 603 (1982); S. Ichimaru, *Physica Scripta*, **T2/1**, 198 (1982).
12. J. Lindhard, Kgl. Danske Videnskab. *Selskab. Mat. Fys. Medd.*, **28**, 8 (1954).
13. Yu. L. Klimontovich and W. D. Kraeft, *Teplofiz. Vys. Temp.*, **12**, 239 (1974).
14. N. W. Ashcroft, *Phys. Lett.*, **23**, 48 (1966).

15. W.-M. Shyu, K. S. Singwi and M. P. Tosi, *Phys. Rev.*, **B3**, 237 (1971); R. Kumaravadivel and R. Evans, *J. Phys.*, **C9**, 3877 (1976); K. N. Khanna and D. P. Khandelwal, *Physica*, **B111**, 291 (1981).
16. J. A. Ascough and N. H. March, *Phys. Chem. Liq.*, **21**, 251 (1990).
17. W. D. Kraeft, D. Kremp and K. Kilimann, *Ann. Phys.*, **29**, 177 (1973).
18. F. Perrot and N. H. March, *Phys. Rev.*, **A41**, 4521 (1990); **A42**, 4884 (1990).
19. L. Reatto, *Phil. Mag.*, **A58**, 37 (1988) and other references there.
20. A. K. Ray, M. W. Johnson, N. H. March and F. Perrot, to be published.